Monsoon reconstructions using bulk and individual foraminiferal analyses in marine sediments offshore India

Kaustubh Thirumalai[1,*] and Steven C. Clemens[2]

[1]Department of Geosciences, University of Arizona, 1040 E, 4th Street Tucson, AZ 85721, USA
[2]Department of Earth, Environmental, and Planetary Sciences, Brown University, 324 Brook Street, Providence, RI 02912, USA

Planktic foraminiferal geochemistry has yielded extensive insights into Cenozoic climate change over timescales ranging from centuries to millions of years. Additionally, recent studies have targeted reconstructing sub-centennial climate signals, including past seasonality, using the stable oxygen isotopic composition (δ^{18}O) in individual tests of planktic foraminifera. Here we assess the signal involved in reconstructing past Indian monsoon strength and seasonality using bulk-foraminiferal and individual foraminiferal analysis (IFA). We focus on three areas offshore India and study the regional sensitivity of foraminiferal carbonate to monsoonal runoff using a forward-model that includes newly re-evaluated relationships between local salinity and seawater-δ^{18}O. We then evaluate the utility of foraminiferal-δ^{18}O across these regions in reconstructing monsoon variability. We find that the foraminiferal-δ^{18}O signal is dominated by processes that control seawater-δ^{18}O variations in the Bay of Bengal versus temperature variations in the Arabian Sea and discuss the implications for the IFA-δ^{18}O signal. Our findings support that both bulk and individual foraminiferal records developed offshore India can provide skilful reconstructions of past monsoon rainfall variability. We conclude that statistical analyses such as that provided in this work can offer useful blueprints to interpreting the relationship between monsoon rainfall and foraminiferal geochemistry.

Keywords: Forward-modelling, individual foraminiferal analysis, palaeomonsoon, Planktic foraminifera.

Introduction

FLUCTUATIONS in Indian monsoon rainfall and the associated anomalies in atmospheric and oceanic circulation significantly influence the socio-economic wellbeing of South Asia[1,2]. Considering ongoing and future trends in greenhouse gas levels, there is a pressing need to anticipate the response of the Indian monsoon to climate forcing and to mitigate uncertainty in model-based projections[3]. In this regard, generation of past hydroclimate records can help characterize the sensitivity of the mean state and variability of monsoon rainfall to well-known forcings in the geological past.

Various marine and terrestrial palaeoclimate archives have been developed to generate records of past monsoon variability. Owing to their ubiquity, preservation and continuous deposition, planktic foraminiferal tests in ocean sediments have become a useful proxy for reconstructing monsoon-related runoff, and hence, monsoon rainfall amount. Planktic foraminifera are microzooplankton that inhabit the upper ocean and secrete calcareous tests (or shells) over their 2–4 week lifespan[4]. The geochemistry of their carbonate tests has proven to be a reliable indicator of past sea-surface conditions and in particular, the stable oxygen isotopic composition (δ^{18}O) of planktic foraminifera is a commonly employed palaeoclimate proxy[5–7]. Foraminiferal δ^{18}O composition is driven by the sea-surface temperature (SST) and the δ^{18}O composition of the water mass within which the organism calcifies[8]. Variations in the local δ^{18}O composition of the seawater are empirically correlated with sea-surface salinity (SSS) owing to similar physical controls: evaporation minus precipitation, advection and freshwater input[9,10]. Thus, the δ^{18}O of seawater has been targeted as a proxy of monsoon runoff, as freshwater and rainwater are significantly depleted in δ^{18}O composition compared to seawater[11,12]. However, foraminiferal δ^{18}O is additionally influenced by changes in SST and as such, removal of the SST influence (e.g. paired Mg/Ca ratios) from the δ^{18}O signal has been used to isolate local δ^{18}O composition of the seawater[13–17]. This paired approach has been employed both in the Bay of Bengal and the Arabian Sea to reconstruct past monsoon variability[18–22].

The time-resolution of sea-surface conditions inferred from foraminiferal geochemistry depends on the sedimentation rate at the core site, typically ranging from centuries to millions of years[23]. This traditional approach involves measurements on multiple planktic foraminiferal tests from a sediment horizon wherein the reconstructed signal represents mean conditions over that time interval. Recently, individual foraminiferal analyses (IFA) has been used to resolve sub-centennial climate signals. Owing to the short monthly lifespan of planktic foraminifera,

*For correspondence. (e-mail: kaustubh@arizona.edu)

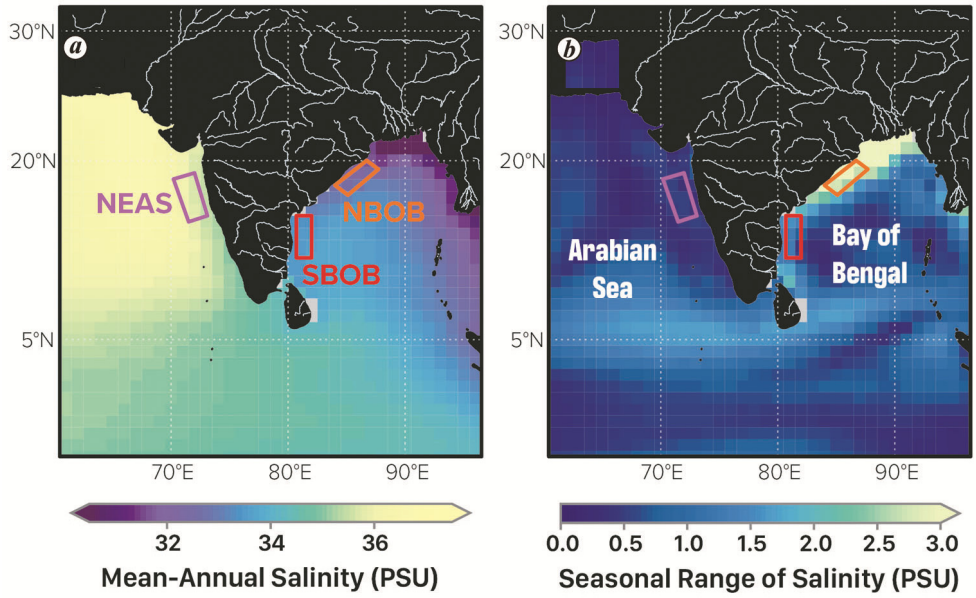

Figure 1. ***a***, Mean annual salinity (PSU) in the northern Indian Ocean with the three chosen regions of study (orange – northern Bay of Bengal; red – southern Bay of Bengal; violet – northeastern Arabian Sea). ***b***, Seasonal range of salinity (PSU) in the northern Indian Ocean. Salinity was obtained from the ORA-S4 reanalysis dataset[31] with the above entities calculated over the entire domain (1958–2013).

IFA represents an estimate of the variability within that time interval[23–28]. In this case, the reconstructed signal can be representative of seasonal, interannual, decadal, or longer forms of climate variability depending on the local climatology as well as foraminiferal environmental preferences (such as calcification depth, habitat, seasonal fluxes, etc.). Apart from these sources of structural uncertainty in the interpretation of IFA, the signal can also be affected by analytical and sampling uncertainty[23,29].

In this study, we assess regional foraminiferal-δ^{18}O signals from the Indian margin using forward-models of carbonate and focus on three regions in the northern Indian Ocean (Figure 1): the Northwestern Bay of Bengal (NBOB; orange), the Southwestern Bay of Bengal (SBOB; red), and the Northeastern Arabian Sea (NEAS; violet). We evaluate the sensitivity of the δ^{18}O signal to monsoon variability and discuss prospects and potential for bulk and individual foraminiferal analyses.

Methods

We forward-model planktic foraminiferal δ^{18}O in space (Figure 1) and time (Figure 2) using monthly gridded SST observations from the HadISST1 dataset[30] (1870–present) and monthly gridded SSS reanalysis data from the ORA-S4 dataset[31] (1958–2013). We focus on modelling carbonate-δ^{18}O for planktic foraminiferal species *Globigerinoides ruber*, a species with photosymbionts (hence thriving in the photic layer), and assume that it calcifies throughout the year and inhabits the upper mixed-layer[32–35]. With these criteria in mind, we focus on the three aforementioned regions (Figure 1) over the 1958–2013 interval (Figure 2). Our analysis can be extended to other species that calcify throughout the year in this zone as well. It can further be improved by focusing on sub-surface dwelling species as well as on foraminifera that occur with a strong seasonal preference[23].

In addition to SST and SSS, forward modelling of foraminiferal carbonate δ^{18}O also requires a relationship between local SSS and seawater-δ^{18}O. Towards this, we subsample measurements made from Ramesh's group at Physical Research Laboratory[11,36] and focus on samples (n = 63) that were collected in the zone of the East India Coastal Current (EICC), which is responsible for transferring low-salinity waters from the Bay of Bengal to the Arabian Sea[37,38]. We develop an EICC-specific seawater-δ^{18}O and SSS equation using these samples and weighted linear regression[39]. We use this equation for the NBOB and SBOB zones and use the prescribed seawater-δ^{18}O-salinity equation according to Singh and others for the near-coastal Arabian Sea region[11].

Our forward model comprises the following equations

$$T = 16.5–4.8\ (\delta^{18}\mathrm{Oc} - \delta^{18}\mathrm{Ow})\ \text{(ref. 8)}$$

$$\delta^{18}\mathrm{Ow} = 0.36(\mathrm{S}) - 12.02\ \text{(EICC developed from Singh } et\ al.^{11}\text{)}\ (r^2 = 0.43;\ P < 0.01)$$

$$\delta^{18}\mathrm{Ow} = 0.26(\mathrm{S}) - 8\ \text{(coastal Arabian Sea from Singh } et\ al.^{11}\text{)}\ (r^2 = 0.62;\ P < 0.01)$$

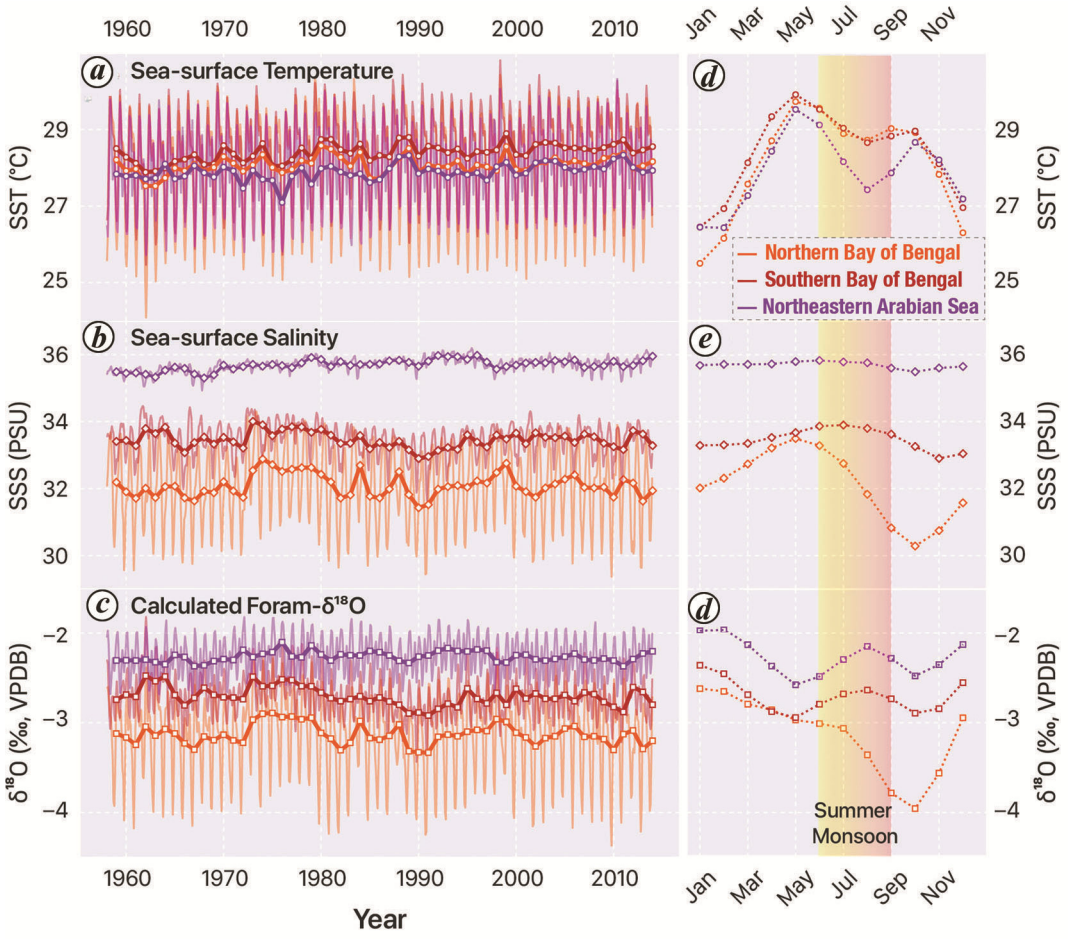

Figure 2. Oceanography of the chosen regions depicting the monthly (thin lines) and annual mean (thick bold lines) sea-surface temperature (SST, °C) (***a***), salinity (SSS, PSU) (***b***), and forward-modelled foraminiferal δ^{18}O (‰, VPDB) (***c***) with their respective climatologies (***d–f***). Colour indicates region of study (orange – northern Bay of Bengal; red – southern Bay of Bengal; violet – northeastern Arabian Sea). SST was taken from the HadISST dataset[30] and SSS from the ORA-S4 dataset[31].

where T is SST, S is SSS, δ^{18}Oc is foraminiferal carbonate δ^{18}O and δ^{18}Ow is the δ^{18}O composition of the seawater.

For comparing forward-modelled planktic foraminiferal-δ^{18}O and monsoon rainfall amount (Figure 3), we use the Global Precipitation Climatology Centre (GPCC) monthly precipitation dataset[40] with 1° lat. × 1° long. resolution. We extract and calculate annual rainfall (in mm/month) from GPCC at grid points adjacent to the oceanic boxes (Figure 1), most representative of their drainage basins: NBOB – Mahandi Basin (19.5°N, 84.5°E); SBOB – Krishna–Godavari Basin (17.5°N, 82.5°E); NEAS – Narmada/Tapti Basin (20.5°N, 73.5°E). We then compare rainfall to annual averages of forward-modelled δ^{18}O (Figure 3 *a–c*) as well as a decadal comparison by computing 10-year centered moving averages.

Finally, to address IFA-δ^{18}O seasonality with relevance to past changes, we statistically vary the seasonal cycle of temperature and salinity by 75% (chosen based on the response of the NBOB seasonal cycle to the complete shutdown of summer monsoon rainfall) and then compare the resulting forward-modelled δ^{18}O to the altered values. Specifically, we inflate and decrease the modern seasonal cycle (Figure 2) in these parameters by 75%. For comparison to the altered values, we utilize quantile–quantile (Q–Q) analysis[25], which is a methodology to compare two different sets of data wherein quantiles of one probability distribution function (PDF) are plotted with another (Figure 4).

Results and discussion

The Bay of Bengal and the Arabian Sea have characteristically different oceanographic patterns (Figures 1 and 2). The seasonal variability of SSS is >3 PSU in the northern Bay of Bengal (Figure 1), dominated by freshening related to summer monsoonal outflow in October (Figure 2 *e*). The SBOB region has a more modest annual cycle of ~1 PSU, with a minima in November, related to a mixture

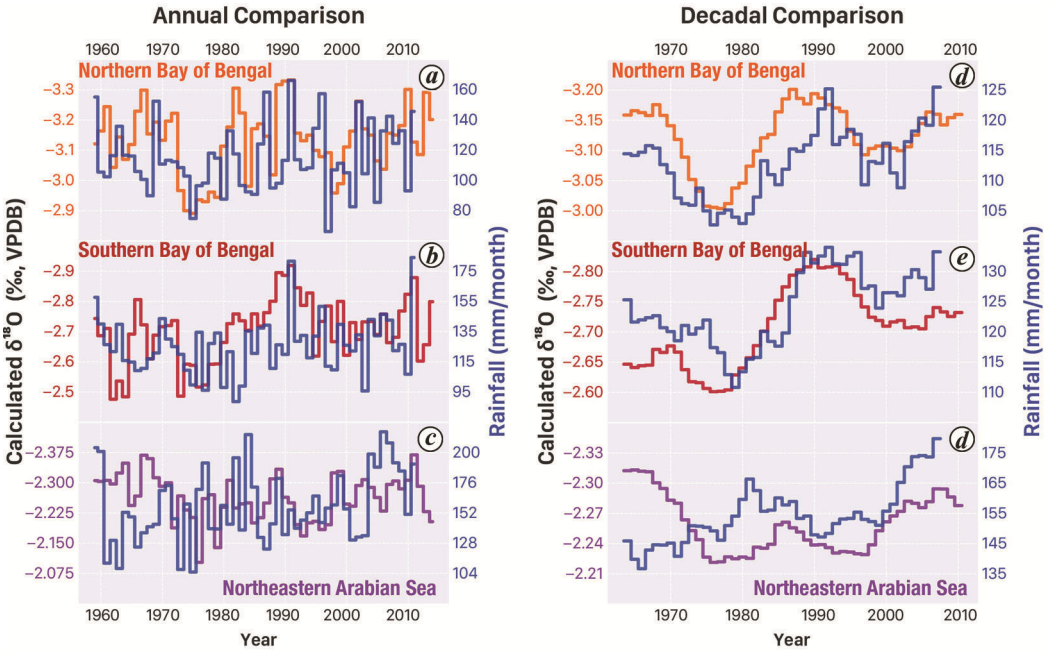

Figure 3. Comparison of annually-averaged (***a–c***) and decadally-averaged (***d–f***) forward-modelled δ^{18}O (‰, VPDB) in oceanic boxes versus precipitation (mm/month) in adjacent catchment areas at the northern Bay of Bengal (orange), southern Bay of Bengal (red), and northeastern Arabian Sea (violet). Precipitation was obtained from the GPCC dataset[40].

of late summer and early winter rains in southeastern India[41], as well as the southward propagation of the EICC carrying low-salinity waters[38]. In sharp contrast, the NEAS experiences a muted seasonal SSS cycle of around 0.5 PSU (Figures 1 and 2). Overall, the Bay of Bengal experiences larger seasonal, interannual and decadal SSS variability than the NEAS region (Figure 2 *b*), driven by freshening during the post-monsoon season. SSS variability in the high-salinity season (or dry season) is restricted even at NBOB ($1\sigma_{\text{May}} = 0.28$ PSU versus $1\sigma_{\text{OCT}} = 0.61$ PSU). Unlike SSS, all three regions experience similar annual mean SST and seasonal variability (~4°C) with relatively minor interannual and decadal variability (Figure 2 *a* and *d*). Although it is notable that SSTs in the NEAS exhibit a pronounced cooling (~1.8°C) within the summer monsoon season (violet line in Figure 2 *d*), which might be indicative of evaporative cooling, runoff of fresher and cooler waters, upwelling, Arabian Sea circulation[42–45], or some combination of these processes. Ultimately, the seasonal evolution of SST and SSS in all these regions is linked to monsoon-related processes.

We find distinct mean states and variability in forward-modelled foraminiferal δ^{18}O that are also tied to the monsoon (Figure 2 *c* and *f*). Forward-modelling helps unravel the dominance of SST versus SSS in controlling the regional δ^{18}O signal. We find that mean annual changes in SSS strongly influence foraminiferal δ^{18}O in both the NBOB and SBOB (compare Figure 2 *c* with *b*), with minor contributions from mean annual SST. Thus, both coastal regions in the Bay of Bengal are ideally suited to develop mean-annual salinity records from bulk-foraminiferal analysis to target past monsoon variability. On the other hand, in the NEAS region, foraminiferal-δ^{18}O is controlled by changes in SST with minimal influence from SSS. It is important to note that SST changes in the Arabian Sea are coupled to monsoon intensity. We also note that available core-top δ^{18}O data of planktic foraminifera from the regions of focus in this study also agree within uncertainty[46]. For example, the core-top value of a core in the NEAS region[5] is ~2‰, whereas one from the SBOB[47] is ~2.5‰, and in NBOB[48] is ~3‰ (Figure 2 *c*). With relevance to bulk-foraminiferal records, we assess the co-variability of the δ^{18}O signal and monsoon rainfall by comparing our forward-modelled values to rainfall in the adjacent drainage basins (Figure 3). There are three major caveats to this exercise: (1) we have chosen rainfall from one grid point in the catchment of the river adjacent to our chosen regions and thus need not be entirely representative of the entire drainage entering the oceanic box, (2) we are comparing gridded observations of rainfall to spatially averaged values derived from gridded, reanalysis datasets precluding a one-to-one comparison, and (3) we are comparing the forward-modelled foraminiferal δ^{18}O signal and not the seawater-δ^{18}O signal. Thus, these comparisons have the potential to be improved in future work. Nevertheless, we find good correspondences between the rainfall and foraminiferal δ^{18}O across the three regions (Figure 3). Although year-to-year anomalies are not always captured (Figure 3 *a–c*), the forward-modelled δ^{18}O tracks long-term rainfall trends (via negative correlations) in all three regions, delineated in the decadal comparison (Figure 3 *d–f*). On

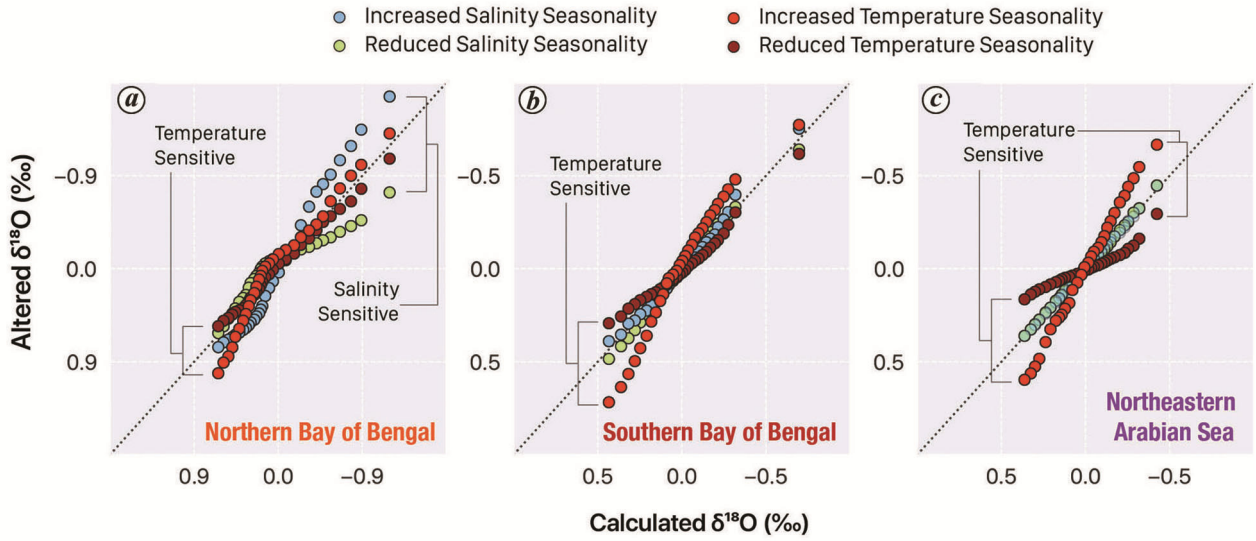

Figure 4. Quantile–quantile (Q–Q) plots of forward-modeled $\delta^{18}O$ at the three sites compared with four cases where SST (increased – orange, decreased – dark red) and SSS (increased – blue, decreased – green) seasonality was altered by a value of 75%. We divided each distribution into 30 quantiles prior to comparison. The 1 : 1 line is also depicted (black dashed line). Note that most extreme values across all regions are more sensitive to temperature change except for the negative extremes in the NBOB region, which respond to changes in seasonality of surface-ocean salinity.

the decadal scale, the match between forward-modelled $\delta^{18}O$ and precipitation improves after 1975, before which the correspondence is poor, possibly due to the lack of salinity observations[31]. Whereas NBOB and SBOB $\delta^{18}O$ are driven by changes in SSS, with lower $\delta^{18}O$ corresponding to stronger rainfall (Figure 3 *a* and *b*), NEAS $\delta^{18}O$ tracks onshore rainfall via associations with temperature (Figure 3 *c* and *f*), where warmer SSTs in the Arabian Sea correspond to greater subcontinental precipitation[42,44,49]. Our analysis suggests that temperature-driven changes over the past 50-years in the NBOB and SBOB region are minimal-to-none and that bulk-foraminiferal $\delta^{18}O$ is directly capable of tracking long-term monsoon rainfall strength (Figure 3 *d* and *e*). We contend that a paired Mg/Ca-$\delta^{18}O$ approach in these regions, with the potential to parse out local seawater-$\delta^{18}O$ (and local SSS) and SST, will yield even more skilled hydroclimate reconstructions of past monsoon strength.

To address the sensitivity of IFA in these regions, we focus on the seasonal cycle of $\delta^{18}O$. In all three regions, year-to-year and longer forms variability in SST and SSS are muted compared to the amplitude of the seasonal cycle. Thus, we alter the seasonality of SST and SSS prior to forward-modelling regional $\delta^{18}O$ and then compare the altered case with the originally calculated signal using Q–Q plots (Figure 4). We increased and reduced the regional SST and SSS seasonal cycle (4 cases) by 75% for this exercise. For context, 75% corresponds to a 3 PSU reduction (i.e. 1 PSU amplitude) in SSS seasonality or a 3°C increase (i.e. 7°C amplitude) in SST seasonality in the NBOB region and a ~0.5 PSU reduction (i.e. ~0.25 PSU amplitude) in SSS seasonality or 3°C increase (i.e. 7°C amplitude) in SST seasonality in the NEAS region.

Our Q–Q analysis shows that the IFA-$\delta^{18}O$ signal exhibits varying spatial sensitivity in the northern Indian Ocean. At the NBOB region, changes in the SSS annual cycle dominate changes in the IFA-$\delta^{18}O$ signal, particularly the extreme quantiles (Figure 4 *a*). Despite large (~1.5°C) increases in warm-season SSTs, changes in the freshwater season control the low-$\delta^{18}O$ extreme quantiles. The high-$\delta^{18}O$ extremes at NBOB are temperature-sensitive and are driven by changes in cold SST minima. Thus, IFA-$\delta^{18}O$ at NBOB is extremely sensitive to changes in monsoon outflow as well as cold-season (winter) SSTs, wherein both aspects are unravelled using Q–Q analyses. Our statistical analysis shows that NBOB is an ideal target to reconstruct past monsoon seasonality and extremes at various time periods.

Compared to the NBOB region, IFA-$\delta^{18}O$ signals at SBOB and NEAS are much less sensitive to changes in SSS seasonality. At SBOB, although there is a minor change in the extreme quantiles with changing SSS seasonality, the sensitivity to SST seasonality is much larger (Figure 4 *b*). Additional work is required to infer whether changes in SST seasonality in SBOB can be objectively tied to monsoonal outflow. In contrast, warmer SSTs in the NEAS region are known to be associated with stronger monsoon winds (Figure 3 *c*); changes in SST seasonality in this region completely dominate the IFA-$\delta^{18}O$ signal (Figure 4 *c*), with SSS sensitivity being minimal-to-none. Thus, IFA-$\delta^{18}O$ at NEAS (and/or other temperature sensitive IFA proxies such as Mg/Ca) via its sensitivity to SST can provide useful insights into past monsoon seasonality.

Conclusion

We have evaluated the sensitivity of planktic foraminiferal-δ^{18}O towards SST, SSS and ultimately, monsoon rainfall in three different regions in the northern Indian Ocean using a forward model. We find that all three regions are suitable for long-term palaeomonsoon reconstructions using bulk, planktic foraminiferal δ^{18}O, which can be further improved by using a paired-approach where the local δ^{18}O of seawater and SST are isolated. In the northern Bay of Bengal, IFA-δ^{18}O is highly sensitive to freshwater runoff during the monsoon and is skilled at reconstructing past monsoon seasonality and extremes. We also find that IFA-δ^{18}O in the northeastern Arabian Sea is sensitive to SST changes and can be targeted for reconstructing monsoon intensity as well. We conclude that forward-modelling statistical exercises offer useful insights to interpreting palaeomonsoon records developed from foraminiferal geochemistry.

1. Gadgil, S., The Indian monsoon, GDP and agriculture. *Econ. Polit. Wkly*., 2006; doi:10.1007/978-94-017-9828-0.
2. Gadgil, S., The Indian monsoon and its variability. *Annu. Rev. Earth Planet. Sci*., 2003; doi:10.1146/annurev.earth.31.100901.141251.
3. Turner, A. G. and Annamalai, H., Climate change and the South Asian summer monsoon. *Nature Clim. Change*, 2012, **2**, 587–595.
4. Spero, H. J., Life history and stable isotope geochemistry of planktonic foraminifera. *Paleontol. Soc. Pap.*, 1998, **4**, 7–36.
5. Sarkar, A., Ramesh, R., Bhattacharya, S. K. and Rajagopalan, G., Oxygen isotope evidence for a stronger winter monsoon current during the last glaciation. *Nature*, 1990, **343**, 549–551.
6. Sarkar, A. *et al*., High resolution Holocene monsoon record from the eastern Arabian Sea. *Earth Planet. Sci. Lett*., 2000, **177**, 1–10.
7. Waelbroeck, C. *et al*., A global compilation of late Holocene planktonic foraminiferal δ^{18}O: relationship between surface water temperature and δ^{18}O. *Quat. Sci. Rev*., 2005, **24**, 853–868.
8. Bemis, B. E., Spero, H. J., Bijma, J. and Lea, D. W., Reevaluation of the oxygen isotopic composition of planktonic foraminifera: experimental results and revised paleotemperature equations. *Paleoceanography*, 1998, **13**, 150–160.
9. Rohling, E. J. and Bigg, G. R., Paleosalinity and δ^{18}O: a critical assessment. *J. Geophys. Res*., 1998, **103**, 1307–1318.
10. Bigg, G. R. and Rohling, E. J., An oxygen isotope data set for marine waters. *J. Geophys. Res. Oceans*, 2000, **105**, 8527–8535.
11. Singh, A., Jani, R. A. and Ramesh, R., Spatiotemporal variations of the δ^{18}O–salinity relation in the northern Indian Ocean. *Deep-Sea Res*., 2010, **57**, 1422–1431.
12. Delaygue, G. *et al*., Oxygen isotope/salinity relationship in the northern Indian Ocean. *J. Geophys. Res*., 2001.
13. Thirumalai, K. *et al.*, Pronounced centennial-scale Atlantic Ocean climate variability correlated with Western Hemisphere hydroclimate. *Nat Commun*., 2018, **9**, 113–111.
14. Clemens, S. C. *et al.*, Precession-band variance missing from East Asian monsoon runoff. *Nature Commun*., 2018, **9**, 1–12.
15. Weldeab, S., Lea, D. W., Schneider, R. R. and Andersen, N., 155,000 years of West African Monsoon and Ocean thermal evolution. *Science*, 2007, **316**, 1303–1307.
16. Oppo, D. W., Rosenthal, Y. and Linsley, B. K., 2000-year-long temperature and hydrology reconstructions from the Indo-Pacific warm pool. *Nature*, 2009, **460**, 1113–1116.
17. Marino, G. *et al*., Agulhas salt-leakage oscillations during abrupt climate changes of the Late Pleistocene. *Paleoceanography*, 2013, **28**, 599–606.
18. Saraswat, R., Nigam, R. and Corrége, T., A glimpse of the Quaternary monsoon history from India and adjoining seas. *Palaeogeogr.*, *Palaeoclim.*, *Palaeoecol*., 2014, **397**, 1–6.
19. Saraswat, R., Lea, D. W., Nigam, R., Mackensen, A. and Naik, D. K., Deglaciation in the tropical Indian Ocean driven by interplay between the regional monsoon and global teleconnections. *Earth Planet. Sci. Lett*., 2013, **375**, 166–175.
20. Anand, P. *et al.*, Coupled sea surface temperature-seawater δ^{18}O reconstructions in the Arabian Sea at the millennial scale for the last 35 ka. *Paleoceanography*, 2008, **23**, PA4207.
21. Rashid, H., Flower, B. P., Poore, R. Z. and Quinn, T. M., A ~25 ka Indian Ocean monsoon variability record from the Andaman Sea. *Quat. Sci. Rev*., 2007, **26**, 2586–2597.
22. Rashid, H., England, E., Thompson, L. G. and Polyak, L., Late Glacial to Holocene Indian Summer Monsoon Variability Based upon Sediment Records Taken from the Bay of Bengal. *Terr. Atmos. Ocean. Sci*., 2011, **22**, 215–214.
23. Thirumalai, K., Partin, J. W., Jackson, C. S. and Quinn, T. M., Statistical constraints on El Niño Southern oscillation reconstructions using individual foraminifera: a sensitivity analysis. *Paleoceanography*, 2013, **28**, 401–412.
24. Naidu, P. D., Niitsuma, N., Thirumalai, K. and Naik, S. S., Significant seasonal contrast in the Arabian Sea during deglaciation evidence from oxygen isotopic analyses of individual planktic foraminifera. *Quat. Int.*, 2018; doi:10.1016/j.quaint.2018.08.005.
25. Ford, H. L., Ravelo, A. C. and Polissar, P. J., Reduced El Niño–Southern oscillation during the last glacial maximum. *Science*, 2015, **347**, 255–258.
26. Leduc, G., Vidal, L., Cartapanis, O. and Bard, E., Modes of eastern equatorial Pacific thermocline variability: Implications for ENSO dynamics over the last glacial period. *Paleoceanography*, 2009, **24**, PA3202.
27. Khider, D., Stott, L. D., Emile-Geay, J., Thunell, R. C. and Hammond, D. E., Assessing El Niño Southern oscillation variability during the past millennium. *Paleoceanography*, 2011, **26**, PA3222.
28. Schmitt, A. *et al*., Single foraminifera Mg/Ca analyses of past glacial-interglacial temperatures derived from *G. rubersensustricto* and sensulato morphotypes. *Chem. Geol*., 2019, **511**, 510–520.
29. Tindall, J. C., Haywood, A. M. and Thirumalai, K., Modeling the stable water isotope expression of El Niño in the Pliocene: implications for the interpretation of proxy data. *Paleoceanography*, 2017, **19**, 191–122.
30. Rayner, N. A. *et al.*, Global analyses of sea surface temperature, sea ice, and night marine air temperature since the late nineteenth century. *J. Geophys. Res*., 2003, **108**, 4407–4437.
31. Balmaseda, M. A., Mogensen, K. and Weaver, A. T., Evaluation of the ECMWF ocean reanalysis system ORAS4. *Quat. J. Roy. Meteorol. Soc*., 2012, **139**, 1132–1161.
32. Thirumalai, K., Richey, J. N., Quinn, T. M. and Poore, R. Z., *Globigerinoides ruber* morphotypes in the Gulf of Mexico: a test of null hypothesis. *Sci. Rep*., 2014, **4**, 1–7.
33. Farmer, E. C., Kaplan, A., de Menocal, P. B. and Lynch-Stieglitz, J., Corroborating ecological depth preferences of planktonic foraminifera in the tropical Atlantic with the stable oxygen isotope ratios of core top specimens. *Paleoceanography*, 2007, **22**, PA3205.
34. Guptha, M. V. S., Curry, W. B., Ittekkot, V. and Muralinath, A. S., Seasonal variation in the flux of planktic Foraminifera; sediment trap results from the Bay of Bengal, northern Indian Ocean. *J. Foraminiferal. Res*., 1997, **27**, 5–19.
35. Richey, J. N. *et al*., Considerations for Globigerinoidesruber (white and pink) paleoceanography: comprehensive insights from

a long-running sediment trap. *Paleoceanogr*., *Paleoclimatol*., 2019.
36. Kumar, P. K. and Ramesh, R., Revisiting reconstructed Indian monsoon rainfall variations during the last ~25 ka from planktonic foraminiferal $\delta^{18}O$ from the Eastern Arabian Sea. *Quat. Int*., 2016, **443**, 1–10.
37. Fousiya, T. S., Parekh, A. and Gnanaseelan, C., Interannual variability of upper ocean stratification in Bay of Bengal: observational and modeling aspects. *Theor. Appl. Climatol*., 2015, 1–17; doi:10.1007/s00704-015-1574-z.
38. Behara, A. and Vinayachandran, P. N., An OGCM study of the impact of rain and river water forcing on the Bay of Bengal. *J. Geophys. Res. Oceans*, 2016, **121**, 2425–2446.
39. Thirumalai, K., Singh, A., Ramesh, R. and Ramesh, R., A MATLAB™ code to perform weighted linear regression with (correlated or uncorrelated) errors in bivariate data. *J. Geol. Soc. India*, 2011, **77**, 377–380.
40. Beck, C., Grieser, J. and Rudolf, B., A new monthly precipitation climatology for the global land areas for the period 1951 to 2000. *Geophys. Res. Abst*., 2005, **7**.
41. Dimri, A. P., Yasunari, T., Kotlia, B. S., Mohanty, U. C. and Sikka, D. R., Indian winter monsoon: Present and past. *Earth Sci. Rev*., 2016, **163**, 297–322.
42. DiNezio, P. N. *et al.*, Glacial changes in tropical climate amplified by the Indian Ocean. *Sci. Adv*., 2018, **4**, eaat9658.
43. Chakravorty, S., Gnanaseelan, C. and Pillai, P. A., Combined influence of remote and local SST forcing on Indian Summer Monsoon Rainfall variability. *Clim. Dyn*., 2016, 1–15; doi:10.1007/s00382-016-2999-5.
44. Murtugudde, R., Seager, R. and Thoppil, P., Arabian Sea response to monsoon variations. *Paleoceanography*, 2007, **22**, 1–17.
45. Prell, W. L. and Streeter, H. F., Temporal and spatial patterns of monsoonal upwelling along Arabia: a modern analogue for the interpretation of Quaternary SST anomalies. *J. Mar. Res.*, 1982.
46. Sijinkumar, A. V. *et al*., $\delta^{18}O$ and salinity variability from the last glacial maximum to recent in the Bay of Bengal and Andaman Sea. *Quat. Sci. Rev.*, 2016, **135**, 79–91.
47. Govil, P., Naidu, P. D. and Kuhnert, H., Variations of Indian monsoon precipitation during the last 32 kyr reflected in the surface hydrography of the Western Bay of Bengal. *Quat. Sci. Rev*., 2011, 1–9; doi:10.1016/j.quascirev.2011.10.004.
48. Kudrass, H. R., Hofmann, A., Doose, H., Emeis, K.-C. and Erlenkeuser, H., Modulation and amplification of climatic changes in the Northern Hemisphere by the Indian summer monsoon during the past 80 kyr. *Geology*, 2001, **29**, 63–65.
49. Tierney, J. E., Pausata, F. S. R. and de Menocal, P. B., Deglacial Indian monsoon failure and North Atlantic stadials linked by Indian Ocean surface cooling. *Nature Geosci.*, 2015, 1–6; doi: 10.1038/ngeo2603.

ACKNOWLEDGEMENTS. We thank Dr Judson Partin (University of Texas at Austin) and Dr Christopher Maupin (Texas A&M University) for helpful discussions on this work. K.T. thanks the National Science Foundation (OCE-1903482) of USA for supporting this work. K.T. acknowledges the pivotal role that Prof. R. Ramesh played in shaping his geoscientific career.

doi: 10.18520/cs/v119/i2/328-334